CrystEngComm

Accepted Manuscript

ROYAL SOCIETY OF CHEMISTRY

www.rsc.org/crystengcomm

CrystEngComm

PAPER

Lanthanide coordination polymers constructed from 5-(1H-tetrazol-5-yl)isophthalic acid ligand: white light emission and color tuning

Received 00th January 20xx,
Accepted 00th January 20xx

DOI: 10.1039/x0xx00000x

www.rsc.org/

Jia Jia[a, b], Jianing Xu[a], Shengyan Wang[a], Pengcheng Wang[a], Lijuan Gao[a], Miao Yu[a], Yong Fan*[a] and Li Wang*[a]

A series of lanthanide coordination polymers (LnCPs), namely $[Ln(TZI)(H_2O)_5]_n$ (**1-5**) (Ln = Nd **1**, Eu **2**, Gd **3**, Tb **4** and Sm **5**), were synthesized through the self-assembly of 5-(1H-tetrazol-5-yl)isophthalic acid (H_3TZI) ligand and lanthanide ions. X-ray crystallographic analysis reveals that compounds **1–5** are isostructural, featuring 1D double-chain structure. The luminescence spectra in the solid state reveal that compouds **2** and **4** exhibit the characteristic luminescence of Eu(III) and Tb(III) ions, respectively, while compound **3** exhibits much enhanced blue-green emission which is derived from H_3TZI ligand. Further, by introducing single dopant Eu(III) and codopants Eu(III)/Tb(III) into the Gd(III) framework, white light emission and color-tunable luminescence from yellow to blue were realized.

Introduction

Full-color luminescent materials, especially those with white light emission, have recently attracted considerable interest because of their potential applications in solid-state lighting, low-cost back-lighting and full color displays.[1–3] However, single-component materials capable of white-light production are rare. The commonly used approach to achieve white light emission is to mix a blue or ultraviolet emitting material with a yellow-emitting phosphor or to blend materials together that can emit red, green, and blue, namely the three primary colors of light.[4-6] Another alternative approach for designing color-tunable and white-light luminescence materials is tuning for the excitation wavelengths[7] of single-component materials[8] or doped materials.[9]

Due to unique optical properties of lanthanide ions, the luminescence from Ln(III) ions is featured by high color purity and long lived excited lifetimes and the emission covers the whole visible range from 400 to 700 nm. Especially, Eu(III) and Tb(III) ions can emit intense red and green light, respectively. Lanthanide coordination polymers (LnCPs) are promising luminescent materials because of the intrinsic physical properties of the Ln(III) ions, such as color-pure luminescence, large paramagnetism, and the fact that the electrostatic nature of their coordination chemistry allows a large variety of symmetries and structural patterns[10–12]. Actually, due to the inner character of their valence orbitals, lanthanide ions have similar chemical properties, and it is possible to synthesize coordination polymers in which two or more lanthanide ions are randomly distributed over the metallic sites.[13,14] This enables one to tune the intermetallic distance and therefore to modulate the color and the brightness of emission.[15–19] Based on the above reasons, LnCPs have attracted more and more interest and been effectively used in the design of multi-color and white-light emitting materials.[20–22] For instance, a new fluorophore that exhibits white light by combining an Eu(III) moiety (red emission) with an organic ligand (blue and green emission) was reported.[8a] Li and co-workers developed a white light emitting compound based on doping Eu(III) ion into the Gd(III) framework for the first time.[23] A combination of blue-emitting ligand/La(III), green-emitting Tb(III) and red-emitting Eu(III) units was utilized to generate white light from La(III)/Tb(III)/Eu(III) coordination polymers.[24]

As known, the selection of appropriate ligands plays a crucial role in the synthesis of LnCPs with promising luminescent properties. The main reason is that organic ligands can be used not only as building blocks for constructing novel frameworks of LnCPs, but also as efficient sensitizers for Ln(III) ions via an "antenna effect".[25] 5-(1H-tetrazol-5-yl)isophthalic acid (H_3TZI) has been validated to be a proper polydentate bridging ligand for the formation of multidimensional coordination polymers exhibiting structural diversity.[26] In addition, H_3TZI ligand is a good antenna for luminescent LnCPs, which exhibits a broad band over a range of 400–580 nm (λ_{max} = 420 nm), in particular in structures where the ligand itself is luminescent, as it is possible to realize an substantial enhancement in intensity and a shift in emission when the ligand is incorporated into a framework structure. So we chose H_3TZI as a

[a] State Key Laboratory of Inorganic Synthesis & Preparative Chemistry, College of Chemistry, Jilin University, Changchun 130012, Jilin, P. R. China. E-mail: lhl222@jlu.edu.cn; Fax: +86-431-85168439; Tel: +86-431-85168439
[b] College of Chemistry, Baicheng Normal University, Baicheng 137000, Jilin, P. R. China. E-mail: jj_zhx@126.com

† Electronic Supplementary Information (ESI) available. CCDC 1028649 for compound 1, 1029007 for compound 2, 1033880 for compound 3, 1028648 for compound 4 and 1029044 for compound 5. For ESI and crystallographic data in CIF or other electronic format see DOI: 10.1039/x0xx00000x

novel ligand to construct lanthanide compounds. As a result, a series of new LnCPs, $[Ln(TZI)(H_2O)_5]_n$ (**1–5**) (Ln = Nd **1**, Eu **2**, Gd **3**, Tb **4**, Sm **5**), which are isostructural, have been isolated and crystallize in triclinic *P*-1 space group consisting of 1D double-chain. With careful adjustment of the relative concentrations of the lanthanide ions and excitation wavelengths, luminescence color of the resulting LnCPs were modulated, and white-light as well as color-tunable emissions was achieved. A sound mechanism for the observed photophysical properties of these LnCPs was also discussed in details.

Experimental

Materials and Methods

All chemicals used in this work were of reagent grade. They were commercially available and used as purchased without further purification. The IR spectra (KBr pellets) were recorded in the range 400–4000 cm^{-1} on a Nicolet Impact 410 spectrometer. Elemental analyses(C, H and N) were performed on an Elementar Vario EL cube CHNOS Elemental Analyzer. Elemental analyses for Eu, Gd, and Tb were obtained using a PLASMA-SPEC(I) ICP atomic emission spectrometer. Thermogravimetric analyses (TGA) were carried out with a PerkinElmer TGA7 instrument, with a heating rate of 10 °C/min under a nitrogen atmosphere(compounds **1–5**) and air atmosphere(compounds **2–4** upon dehydration), respectively. Powder X-ray diffraction (XRD) measurements were performed with a SHIMADZU XRD-6000 diffractometer with Cu-Kα radiation (λ = 1.5418 Å) in the 2θ range of 4–40°. Photoluminescence spectra were obtained by an Edinburgh Instruments FLS 920 spectrophotometer. The Commission International de l'Eclairage (CIE) color coordinates were calculated by following the international CIE standards.[27]

Synthesis of $[Ln(TZI)(H_2O)_5]_n$ (1–5) (Ln = Nd 1, Eu 2, Gd 3, Tb 4, Sm 5)

All compounds including the doped-lanthanide ones were obtained by adopting an otherwise identical procedure except for the different starting lanthanide salts. The synthesis of $[Eu(TZI)(H_2O)_5]_n$ (**2**) is thus presented here in detail as a representative: A mixture of $Eu(NO_3)_3{\cdot}6H_2O$ (44.6 mg, 0.1 mmol), H_3TZI (23.4 mg, 0.1 mmol), and 2,2'-bipy (15.6 mg, 0.1 mmol) were dispersed in H_2O (8 mL), and then 0.5 mL of 0.1M NaOH was added into the mixture to adjust pH = 4.0. Finally, the mixture solution was transferred into a 15 mL Teflon-lined autoclave and heated at 150 °C under autogenous pressure for three days, then cooled to room temperature under ambient conditions. Block crystals of compounds **1–5** were recovered by filtration, washed with distilled water, and dried in air. Yield: 56% for **1**, 68% for **2**, 62% for **3**, 58% for **4** and 65% for **5** (based on H_3TZI ligand). Element analysis (%) for **1**, calcd: C 23.22, H 2.82, N 12.04; found: C 23.46 , H 2.85, N 12.16. IR data (KBr pellet cm^{-1}): 3437(s), 2925(w), 1628(m), 1555(m), 1490(w), 1446(w), 1394(s), 1351(w), 786(w), 754(w), 701(w), 565(w), 488(w). Element analysis (%) for **2**, calcd: C 22.85, H 2.77, N 11.84; found: C 23.04, H 2.70, N 12.02. IR data (KBr pellet cm^{-1}): 3443(s), 2926(m), 1624(w), 1546(m), 1500(w), 1442(w), 1391(s), 1345(w), 788(w), 757(w), 701(m), 565(w), 488(m). Element analysis (%) for **3**: calcd: C 22.59, H 2.74, N 11.71; found: C 22.84, H 2.75, N 11.86. IR data (KBr pellet cm^{-1}): 3452(s), 2928(w), 1625(m), 1552(m), 1500(w), 1441(w), 1391(s), 1345(w), 788(w),757(w), 702(m), 565(w), 488(w). Element analysis (%) for **4**, calcd: C 22.51, H 2.73, N 11.67; found: C 22.77, H 2.76, N 11.80. IR data (KBr pellet cm^{-1}): 3434 (s), 2928(w), 1625(m), 1552(m), 1500(w), 1442(w), 1391(s), 1345(w), 788(w), 757(w), 700(w), 565(w), 489(w). Element analysis (%) for **5**, calcd: C 22.92, H 2.78, N 11.88; found: C 23.14, H 2.84, N 11.97. IR data (KBr pellet cm^{-1}): 3441 (s), 2922(w), 1624(m), 1547(m), 1499(w), 1441(w), 1386(s), 1345(w), 788(w), 757(w), 702(w), 564(w), 488(w).

Synthesis of $[Eu_{0.10}Gd_{0.90}(TZI)(H_2O)_5]_n$ (6) and $[Eu_{0.15}Gd_{0.70}Tb_{0.15}(TZI)(H_2O)_5]_n$ (7)

For the isostructural Eu(III) or Eu(III)/Tb(III) codoped Gd(III) framework, the synthetic method is same as mentioned above just by loading the corresponding $Eu(NO_3)_3{\cdot}6H_2O$ and $Gd(NO_3)_3{\cdot}5H_2O$ or $Eu(NO_3)_3{\cdot}6H_2O$, $Tb(NO_3)_3{\cdot}6H_2O$ and $Gd(NO_3)_3{\cdot}5H_2O$ as the starting materials in stoichiometric ratios. Yield: 62% for **6** (based on H_3TZI ligand). IR data (KBr pellet cm^{-1}): 3609(w), 3497(w), 3405 (s), 1623(m), 1605(w), 1583(w), 1546(m), 1500(w), 1447(w), 1393(s), 788(w), 756(w), 716(w), 565(w), 507(w). Yield: 60% for **7** (based on H_3TZI ligand). Selected IR data (KBr pellet cm^{-1}): 3607(w), 3496(w), 3408(s), 2924(b), 1625(m), 1606(w), 1550(m), 1500(w), 1444(w), 1392(s), 1346(w), 788(w), 757(w), 703(w), 565(w), 488(w).

The doped LnCPs **8–12** were synthesized using the same method as that of **7**. The starting molar ratios of Eu(III) / Gd(III) / Tb(III) in the resulting materials were listed in Table 1. Analyses of the relative molar concentration of the individual lanthanide elements are consistent with the corresponding ratios in the starting codopants (Table 2).

Table 1 Molar ratios of multi-component Eu(III) / Gd(III) / Tb(III) for compounds **8–12**.

Compounds	Eu(III)	Gd(III)	Tb(III)
8	0.25	0.70	0.05
9	0.20	0.70	0.10
10	0.25	0.60	0.15
11	0.20	0.55	0.25
12	0.25	0.50	0.25

Table 2 Elemental analyses (ICP) for compounds **6–12**.

Molar ratio of Eu:Gd:Tb	Wt% Eu Calcd (Found)	Wt% Gd Calcd (Found)	Wt% Tb Calcd (Found)
10%:90%:0% (**6**)	9.90 (9.68)	90.10 (90.32)	0
15%:70%:15% (**7**)	14.85 (14.58)	70.08 (70.41)	15.07 (15.01)
25%:70%:5% (**8**)	24.79 (24.52)	70.18 (70.34)	5.03 (5.14)
20%:70%:10% (**9**)	19.82 (19.96)	70.13 (70.28)	10.05 (9.76)
25%:60%:15%(**10**)	24.78 (24.49)	60.13 (60.35)	15.09 (15.16)
20%:55%:25%(**11**)	19.81 (19.46)	55.07 (55.26)	25.12 (25.28)
25%:50%:25%(**12**)	24.77 (24.98)	50.09 (50.24)	25.14 (24.78)

X-ray crystallography

The crystal data of compounds **1–5** were acquired on a Rigaku R-AXIS RAPID diffractometer equipped with graphite-monochromated Mo-Kα (λ = 0.71073 Å) radiation in the ω scanning mode at room temperature. All structures were solved by direct methods and refined using full-matrix least-squares techniques with the SHELXTL software package.[28] All non-hydrogen atoms were refined anisotropically and the hydrogen atoms were placed in fixed, calculated positions using a riding model. Selected crystallographic data and refinement parameters of compounds **1–5** are listed in Table S1, and the selected bond lengths and angles data are presented in Table S2.

Results and discussion

Structural descriptions

The compounds $[Ln(TZI)(H_2O)_5]_n$ (**1–5**) (Ln = Nd **1**, Eu **2**, Gd **3**, Tb **4**, Sm **5**) crystallize in triclinic *P*-1 space group and are isostructural, as such only the structure of **1** is discussed in detail as a representive. Each Nd(III) ion is eight-coordinated in the coordination geometry of a trigonal dodecahedron (Fig. S1a) by three oxygen atoms from three different TZI^{3-} ligands and five oxygen atoms from the water molecules (Fig. 1a). The bond distance of Nd–O varies from 2.360(3) to 2.529(3) Å. The inversion-related planes of benzene ring in TZI^{3-} ligand are completely parallel (dihedral angle is 0° and the distance of centroid is 3.511 Å), giving rise to an intramolecular π–π stacking interaction. Two adjacent Nd(III) ions are connected by carboxylate of TZI^{3-} ligands giving rise to binuclear SBU (Fig. S1b). The TZI^{3-} anion connects the binuclear SBUs through a bidentate carboxylate group and a monodentate carboxylate group forming 1D double-chain structure (Fig. 1b). The Nd···Nd distances are 5.455 and 9.813 Å when Nd(III) ions are in the adjacent chain or in the same chain. The 1D double chains are linked by O(5)–H(5)···O(4), O(6)–H(7)···N(4) and O(7)–H(1)···O(4) hydrogen bonds forming 2–D structure (Fig. S1c). The hydrogen bond lengths and bond angles are listed in Table S3. It should be noted that the hydrogen bonds and π–π stacking interactions can play an important role in stabilizing the structure of the polymer. Also, two adjacent networks are further linked together by O(5)–H(6)···N(1) and O(9)–H(3)···N(2) hydrogen bonds to form a 3–D supramolecular structure (Fig. S1d).

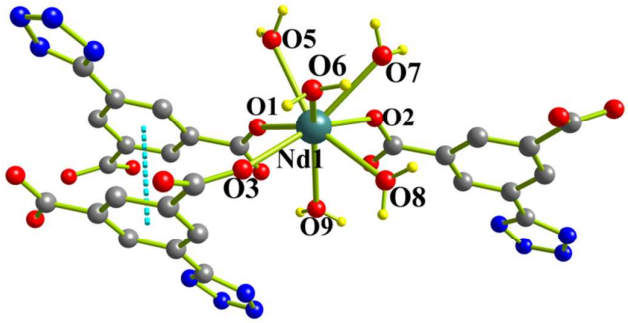

(a)

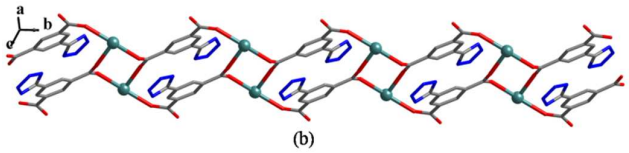

(b)

Fig. 1 (a) The coordination environment of the Nd(III) ion and intra π–π stacking interaction in **1**; (b) 1D double-chain in **1** (coordinated water molecules are omitted for clarity).

Characterization

The IR spectra of compounds **1–5** show similarities (Fig. S2). There is a broad band at 3300-3600 cm^{-1}, which should be ascribed to the stretching vibrations of O–H, suggesting the presence of free or coordinated water molecules. The peaks 1400–1500 cm^{-1} indicate the existence of tetrazole groups.[29] The IR spectrum of the H_3TZI ligand evidences two intense bands at approximately 1695 and 1430 cm^{-1}, which are attributable to the anti-symmetric υ_{as}(C=O) and symmetric υ_s(C=O) vibration modes, respectively. In the cases of the IR spectra of **1–5**, both of these C=O vibrational modes are shifted to lower wave numbers and split into two peaks (1628, 1555 cm^{-1} and 1394, 1351 cm^{-1} in **1**; 1624, 1546 cm^{-1} and 1391, 1345 cm^{-1} in **2**; 1625, 1552 cm^{-1} and 1391, 1345 cm^{-1} in **3**; 1625, 1552 cm^{-1} and 1391, 1345 cm^{-1} in **4**, 1624, 1547 cm^{-1} and 1386, 1345 cm^{-1} in **5**), thus indicating coordination of the carbonyl oxygen to the Ln(III) cations. This coordination is further supported by the appearance of band at 488 cm^{-1} due to Ln-O stretching vibrations.[30] Furthermore, the IR spectra of these compounds exhibit a separation of the asymmetric and symmetric stretching vibrations [$\Delta\upsilon_{(C=O)} = \upsilon_{as} - \upsilon_s$] at approximately 234 and 204 cm^{-1} for **1**, 233 and 201cm^{-1} for **2**, 234 and 207cm^{-1} for **3**, 234 and 207cm^{-1} for **4**, 238 and 202cm^{-1} for **5**, which implies coordination of the carboxylate groups to the Ln(III) cation in a bidentate bridging and monodentate mode in each case.[9c, 9d, 31-33]

Powder X-ray diffraction patterns of these compounds **1–5** are in agreement with the simulated ones based on the corresponding single-crystal structural analysis, which further suggests the purity of the bulk crystalline products. As can be seen from Fig. S3, the doped LnCPs **6–12** are also isostructural to their single lanthanide analogues.

Thermogravimetric analysis (TGA) of the LnCPs was carried out between 25–800 °C. The TGA curves of compounds **1–5** are similar (Fig. S4), so the curve of **5** is discussed as a representation. The first step from 25 °C to 200 °C corresponds to the removal of the five coordinated water molecules (weight loss ca. 18.35%, calculated 19.10%). The framework starts decomposing at about 400 °C. The framework is not decomposed completely in the nitrogen atmosphere up to 800 °C. Importantly, our LnCPs demonstrate an excellent hydrothermal stability. Treating the crystalline compound with boiling water for 24 h does not result in loss of crystallinity (Fig. S5). This is uncommon, as most LnCPs are unstable at high humidity. The stability is due to the face-to-face arrangement

of the TZI^{3-} ligand within the SBUs. Such structural stability against water is rarely seen in LnCPs.[34–38]

Before performing the experiments of luminescence, compounds **2–4** were activated by heating the samples at 120 °C for 48 h in vacuum oven. The XRD patterns and the TGA curves of the activated compounds **2–4** confirm the retention of the framework after the loss of the five coordinated water molecules (Fig. S6 and Fig. S7).

Photoluminescence properties

Solid state luminescence spectra of the H_3TZI ligand and compounds **2–5** were recorded at room temperature as shown in Fig. 2 and the excitation spectra of compounds **2–5** are shown in Fig. S8. Upon excitation at 350 nm, the free H_3TZI ligand exhibits a blue light emission at 420, 437 and 480 nm due to π→π* transitions of the ligand (Fig. 2a insert). However, compound **3** exhibits much enhanced blue-green emission and the red shifts to 448, 495 and 525 nm with the excitation at 358 nm in comparison to the band of the free ligand (Fig. 2b). It is known that the energies of the excited levels of the Gd(III) ion are much higher than the typical energy of the ligand triplet states, inhibiting any ligand-to-metal energy transfer process.[39] The enhancement and the red shifts respectively of the emission band in compound **3** are attributed to the coordination of TZI^{3-} ligands to metal ions, which has enabled the rigidity of the aromatic backbones and thus reduces the loss of energy by radiationless decay of the intraligand emission excited state.[7a,40] The decay curve (Fig. S9b) for compound **3** monitored at 495 nm (λex = 358 nm) can be well fitted into a double exponential function as $I = I_0 + A_1 \exp(-t/\tau_1) + A_2 \exp(-t/\tau_2)$ (where τ_1 and τ_2 are defined as the luminescent lifetimes): τ_1 = 1.174 ms and τ_2 = 6.497 ms. The obtained effective lifetime of compound **3** is increased comparing with the lifetime of the free ligand (τ_1 = 0.610 ns and τ_2 = 2.598 ns) (Fig. S9e).

When excited at 352nm, compound **2** emitted characteristic red luminescence of the Eu(III) and the emission spectrum has five characteristic bands at 578($^5D_0 \rightarrow {}^7F_0$), 594 ($^5D_0 \rightarrow {}^7F_1$), 614 ($^5D_0 \rightarrow {}^7F_2$), 652 ($^5D_0 \rightarrow {}^7F_3$) and 688–700 ($^5D_0 \rightarrow {}^7F_4$) nm, respectively (Fig. 2a). The emission intensity of $^5D_0 \rightarrow {}^7F_2$ (614 nm) is much higher than that of $^5D_0 \rightarrow {}^7F_1$ (594 nm). The decay curve (Fig. S9a) for compound **2** (monitored by $^5D_0 \rightarrow {}^7F_2$, 614 nm) can be well fitted into a mono-exponential function as $I = I_0 + A_1 \exp(-t/\tau)$ (where τ is defined as the luminescent lifetimes): τ = 152.7 μs. As shown in Fig. 2c, under excitation at 322nm, compound **4** emitted the characteristic green luminescence of Tb(III), with four characteristic bands at 487 ($^5D_4 \rightarrow {}^7F_6$), 543 ($^5D_4 \rightarrow {}^7F_5$), 583 ($^5D_4 \rightarrow {}^7F_4$), and 620 ($^5D_4 \rightarrow {}^7F_3$) nm. The most intense emission at 543 nm is attributed to the $^5D_4 \rightarrow {}^7F_5$ transition of the Tb(III) ion. The decay curve (Fig. S9c) for compound **4** (monitored by $^5D_4 \rightarrow {}^7F_5$, 543 nm) was well fitted to a mono–exponential function: $I = I_0 + A_1 \exp(-t/\tau)$, τ = 639.3μs. The characteristics of luminescent emission in compounds **2** and **4** indicate that the antenna effect occurs, that is, energy migration takes place upon ligand absorption, followed by intersystem crossing S1→T1 and antenna T1→f transfer, and then generating f–f emissions of Eu(III) and Tb(III) ions. No broad emission band resulting from the ligand is observed in compounds **2** and **4**, indicating that the energy transfer from the ligands to Eu(III) and Tb(III) centers is very effective.[5d]

Upon excitation at 353nm, compound **5** displays a series of characteristic narrow band emissions of Sm(III) ions at 597nm, 642nm and 706nm, corresponding to the $^4G_{5/2} \rightarrow {}^6H_{7/2}$, $^4G_{5/2} \rightarrow 6H_{9/2}$, and $^4G_{5/2} \rightarrow {}^6H_{11/2}$ transitions(Fig. 2d). In addition, the emission bands of the ligand are also observed (512nm), which indicates that the energy transfer from the ligand to the metal center is not complete. The lifetime values with a double exponential curve (Fig. S9d) are τ_1 = 0.615 ns and τ_2 = 3.195 ns, respectively.

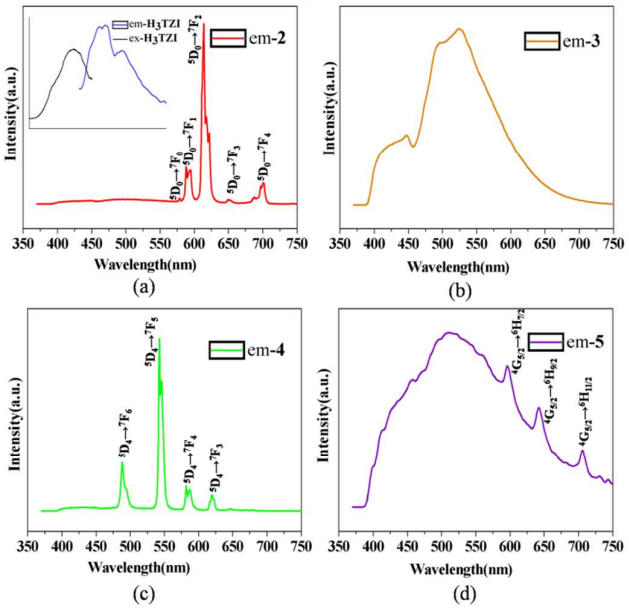

Fig. 2 Solid-state emission spectra of (a) Eu-**2**, (b) Gd-**3**, (c) Tb-**4** and (d) Sm-**5** at room temperature. Insert: Solid-state emission and excitation spectra of H_3TZI

Color-tunable luminescence

Since compounds **2** and **3** are isostructural and emit red and blue-green light, respectively, it may construct the white-light emitting materials through doping Eu(III) ions into the Gd(III) framework by precisely controlling the concentration profiles of Gd/Eu and excitation wavelengths. As such, the Eu(III)-doped Gd(III) compound $Eu_{0.10}$ $Gd_{0.90}$ (compound **6**) has been synthesized and its phase purity was verified by PXRD analysis (Fig. S3). The emission spectra of the compound $Eu_{0.10}$ $Gd_{0.90}$ were recorded under varying UV light excitation from 330 to 380 nm (Fig. 3a). The emission spectra of Eu(III)-doped Gd(III) materials exhibit a broad emission band in the region of 400 to 550 nm of the ligands in compound **3** and the characteristic emission peaks centered at 578, 594, 614, 652, and 688–700 nm of the Eu(III) ion in compound **2**.

With the increase in excitation wavelength, the relative intensity of blue-green emissions gradually increases and at the same time the red emissions decrease. As a result, white emission emerges upon excitation at 350-380 nm. When excited at 350nm, the CIE coordinate (0.332, 0.294) is near to the pure white value (0.333, 0.333) and the quantum yield is 2.81%. The current concept of excitation dependent photoluminescence tuning in the blue, yellowish red and white regions is controlled by different energy transfer processes. In the case of higher energy absorption, the usual "antenna effect" dominates, which generates a yellowish red light emission. Furthermore, when the absorbed energy is too low to allow intersystem crossing to occur, the ligand fluorescence in the blue region dominates. Thus, a white light emission can be realized through a combination of the usual triplet pathway and a ligand fluorescence process, when an intermediate energy is absorbed.[9c,9d,41] The emission colors at different excitation wavelengths are illustrated in the CIE chromaticity diagram (Fig. 3b), whilst the corresponding CIE color coordinates are listed in Table S4.

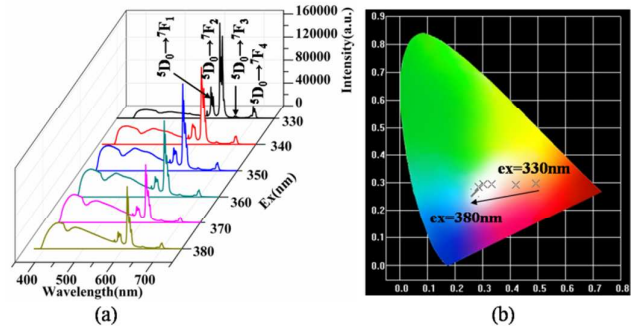

Fig. 3(a) Solid-state emission spectra of compound $Eu_{0.10}$ $Gd_{0.90}$ with excitation wavelengths varying from 330 to 380 nm. (b) The CIE chromaticity diagram for the compound $Eu_{0.10}$ $Gd_{0.90}$ under excitation wavelengths from 330 to 380 nm.

By precisely controlling the concentration profiles of Gd/Eu/Tb and excitation wavelengths, white light emissions were obtained. The emission profiles of doped lanthanide compounds **8–12** excited at 365 nm are depicted in Fig. 4a. The doped lanthanide compounds consisting of multiple luminescent dopants display mixed emission patterns with different relative peak intensities depending on the ratios of the Tb(III), Eu(III) and Gd(III) ions, resulting in the white light emission. The calculated chromaticity coordinates (Table S5) all fall within the white-light region of the 1931 CIE chromaticity diagram (for pure white x = 0.333, y = 0.333). It has been found that compound **12** nearly pure white light emission was achieved with its CIE coordinate of (0.336, 0.325). The quantum yields of **8–12** are 5.28%, 9.25%, 2.88%, 2.92% and 9.75%, respectively. The emission colours for **8–12** are illustrated in the CIE chromaticity diagram (Fig. 4b).

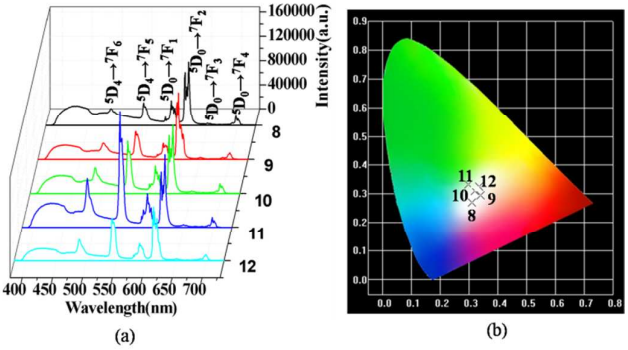

Fig. 4 (a) Solid-state emission spectra of compounds **8–12** with excitation wavelengths at 365 nm . (b) The CIE chromaticity diagram for the compounds **8–12** under excitation wavelengths at 365 nm.

The emission spectra of the compound $Eu_{0.15}$ $Gd_{0.70}$ $Tb_{0.15}$ (compound **7**) were recorded under varying UV light excitation from 320 to 394 nm (Fig. S10a). Strikingly, tunable colors and white light have been observed along with varying excitation wavelengths. When excited at 320 and 330 nm, the compound $Eu_{0.15}$ $Gd_{0.70}$ $Tb_{0.15}$ mainly emits intense yellow luminescence. Upon varying the excitation light to 340 nm, the emission displays green light, and adjusting the excitation light from 350 to 390 nm, it mainly displays blue light. When excited at 394nm, near white light emission is obtained and its CIE coordination is (0.314, 0.244). The quantum yield is 3.83%. The emission colors at different excitation wavelengths are illustrated in the CIE chromaticity diagram (Fig. S10b), while the corresponding CIE color coordinates are listed in Table S6.

The luminescence emission decay measurements were performed for doped compounds **6–12** at room temperature. The decay curves for the compounds are well fitted into a double exponential function: $I = I_0 + A_1 \exp(-t/\tau_1) + A_2 \exp(-t/\tau_2)$, where τ_1 and τ_2 are defined as the luminescent lifetimes. The detailed fitting results are summarized in Table S7. As shown in Fig. S11, the PL decay curve of compounds **6–12** are recorded at room temperature with emission monitored by the $^5D_4 \rightarrow {}^7F_5$ transition at 543 nm and the $^5D_0 \rightarrow {}^7F_2$ transition at 614 nm (λ_{ex} = 365 nm).

Conclusions

In summary, a series of new LnCPs, namely $[Ln(TZI)(H_2O)_5]_n$ (**1–5**) (Ln = Nd **1**, Eu **2**, Gd **3**, Tb **4** and Sm **5**), has been synthesized under hydrothermal conditions. They are isostructural, featuring 1D double-chain structure. Considering compound **3** emits blue-green light, it can be used as a parent framework. Through doping Eu(III) ions into the Gd(III) framework, and by precisely controlling the concentration profiles of Gd/Eu together with varying the excitation wavelengths, white-light emitting materials were obtained. In addition, through the doping of Eu(III)/Tb(III) into the Gd(III) framework, white light emission and tunable colors from yellow to blue have been observed. The synthesis of other

luminescence functional LnCPs constructed from azolate-carboxylic acid derivatives is underway.

Acknowledgements

We gratefully acknowledge the financial support through the National Nature Science Foundation of China (no. 21171065 and 21201077) and the Open Project of Key Laboratory (2013-25) (State Key Laboratory of Inorganic Synthesis & Preparative Chemistry, College of Chemistry, Jilin University, Changchun 130012, Jilin, P. R. China).

Notes and references

1 (a) L. Kreno, K. Leong, O. Farha, M. Allendorf, R. Duyne and J. Hupp, *Chem. Rev.*, 2012, **112**, 1105; (b) S. Reineke, F. Lindner, G. Schwartz, N. Seidler, K. Walzer, B. Lussem and K. Leo1, *Nature*, 2009, **459**, 234; (c) B. W. D'Andrade and S. R. Forrest, *Adv. Mater.*, 2004, **16**, 1585; (d) C. Y. Sun, X. L. Wang, X. Zhang, C. Qin, P. Li, Z. M. Su, D. X. Zhu, G. G. Shan, K. Z. Shao, H. Wu and J. Li, *Nat. Commun.*, 2013, **4**, 2717.

2 (a) Y. C. Zhu, L. Zhou, H. Y. Li, Q. L. Xu, M. Y. Teng, Y. X. Zheng, J. L. Zou, H. J. Zhang and X. Z. You, *Adv. Mater.*, 2011, **23**, 4041; (b) G. M. Farinola and R. Ragni, *Chem. Soc. Rev.*, 2011, **40**, 3467.

3 (a) Y. Liu, M. Pan, Q. Yang, L. Fu, K. Li, S. Wei and C. Su, *Chem. Mater.*, 2012, **24**, 1954; (b) H. C. Su, H. F. Chen, F. C. Fang, C. C. Liu, C. C. Wu, K. T. Wong, Y. H. Liu and S. M. Peng, *J. Am. Chem. Soc.*, 2008, **130**, 3413;(c) Y. H. Niu, M. S. Liu, J. W. Ka, J. Bardeker, M. T. Zin, R. Schofield, Y. Chi and A. K. Y. Jen, *Adv. Mater.*, 2007, **19**, 300; (d) S. Saha, G. Das, J. Thote, and R. Banerjee, *J. Am. Chem. Soc*., 2014, **136**, 14845.

4 E. F. Schubert and J. K. Kim, *Science,* 2005, **308**, 1274.

5 (a) X. H. Zhu, J. Peng, Y. Cao and J. Roncali, *Chem. Soc. Rev.*, 2011, **40**, 3509; (b) Z. Y. Mao and D. J. Wang, *Inorg. Chem*., 2010, **49**, 4922; (c) C. H. Huang and T. M. Chen, *Inorg. Chem.*, 2011, **50**, 5725; (d) X. Rao, Q. Huang, X. Yang, Y. Cui, Y. Yang, C. Wu, B. Chen and G. Qian, *J. Mater. Chem.*, 2012, **22**, 3210.

6 (a) H. Sasabe, J. Kido, *Chem. Mater.,* 2011, **23**, 621. (b) J. Liu, Q. Yang, L. Zhang, D. Jiang, X. Shi, J. Yang, H. Zhong and C. Li, *Adv. Funct. Mater.*, 2007, **17**, 569.

7 (a) Y. Cui, Y. Yue, G. Qian and B. Chen, *Chem. Rev.*, 2012, **112**, 1126; (b) J. Kai, M. C. F. C. Felinto, L. A. O. Nunes, O. L. Malta and H. F. Brito, *J. Mater. Chem.*, 2011, **21**, 3796; (c) C. Shi, H. Sun, X. Tang, W. Lv, H. Yan, Q. Zhao, J. Wang and W. Huang, *Angew. Chem., Int. Ed.*, 2013, **125**, 13676; (d) L. Liang, W. Wang, J. Wu, F. Xu, Y. Niu, B. Xu and P. Xu, *Chem. – Eur. J.*, 2013, **19**, 13774.

8 (a) G. J. He, D. Guo, C. He, X. L. Zhang, X. W. Zhao and C. Y. Duan, *Angew. Chem., Int. Ed.*, 2009, **48**, 6132; (b) M. S. Wang, S. P. Guo, Y. Li, L. Z. Cai, J. P. Zou, G. Xu, W. W. Zhou, F. K. Zheng and G. C. Guo, *J. Am. Chem. Soc.*, 2009, **131**, 13572; (c) A. Balamurugan, M. L. P. Reddy and M. Jayakannan, *J. Physical Chemistry B*, 2009, **113**, 14128.

9 (a) S. M. Li, X. J. Zheng, D. Q. Yuan, A. Ablet and L. P. Jin, *Inorg. Chem.*, 2012, **51**, 1201; (b) K. Liu, H. You, Y. Zheng, G. Jia, Y. Huang, M. Yang, Y. Song, L. Zhang and H. Zhang, *Cryst. Growth Des*., 2009, **10**, 16; (c) A. R. Ramya, S. Varughese and M. L. P. Reddy, *Dalton Trans.*, 2014, **43**, 10940; (d) J. Q. Zhang, H. F. Li, P. Chen, W. B. Sun, T. Gao and P. F. Yan, *J. Materials Chemistry C*, 2015, **3**, 1799; (e) Z. F. Liu, M. F. Wu, S. H. Wang, F. K. Zheng, G. E. Wang, J. Chen, Y. Xiao, A. Q. Wu, G. C. Guo and J. S. Huang, *J. Mater. Chem. C*, 2013, **1**, 4634.

10 T. M. Reineke, M. Eddaoudi, M. Fehr, D. Kelley and O. M. Yaghi, *J. Am. Chem. Soc.,* 1999, **121**, 1651.

11 T. M. Reineke, M. Eddaoudi, and O. M. Yaghi, *Angew. Chem. Int. Ed*., 1999, **38**, 2590.

12 K. A. White, D. A. Chengelis, K. A. Gogick, J. Stehman, N. L. Rosi, and S. Petoud, J. *Am. Chem. Soc*., 2009, **131**, 18069.

13 N. Kerbellec, D. Kustaryono, V. Haquin, M. Etienne, C. Daiguebonne, and O. Guillou, *Inorg. Chem*., 2009, **48**, 2837.

14 V. Haquin, F. Gumy, C. Daiguebonne, J. C. G. Bünzli and O. Guillou, *Eur. J. Inorg. Chem.*, 2009, **29-30**, 4491.

15 V. Haquin, M. Etienne, C. Daiguebonne, S. Freslon, G. Calvez, K. Bernot, L. L. Pollès, S. E. Ashbrook, M. R. Mitchell, J. C. G. Bünzli, S. V. Eliseeva and O. Guillou, *Eur. J. Inorg. Chem.*, 2013, **20**, 3464.

16 S. Dang, J. H. Zhang and Z. M. Sun, *J. Mater. Chem*., 2012, **22**, 8868.

17 M. O. Rodrigues, J. D. L. Dutra, L. A. O. Nunes, G. F. de Sá, W. M. de Azevedo, P. Silva, F. A. A. Paz, R. O. Freire and S. A. Júnior, *J. Phys. Chem. C*, 2012, **116**, 19951.

18 F. L. Natur, G. Calvez, C. Daiguebonne, O. Guillou, K. Bernot, J. Ledoux, L. L. Pollès and C. Roiland, *Inorg. Chem*., 2013, **52**, 6720.

19 S. Biju, D. B. A. Raj, M. L. P. Reddy, C. K. Jayasankar, A. H. Cowley and M. Findlater, *J. Mater. Chem*., 2009, **19**, 1425.

20 (a) S. Sivakumar, F. C. J. M. van Veggel and M. Raudsepp, *J. Am. Chem. Soc.*, 2005, **127**, 12464; (b) J. Xu, L. Jia, N. Jin, Y. Ma, X. Liu, W. Wu, W. Liu, Y. Tang and F. Zhou, *Chem. –Eur. J.*, 2013, **19**, 4556; (c) J. C. Rybak, M. Hailmann, P. R. Matthes, A. Zurawski, J. Nitsch, A. Steffen, J. G. Heck, C. Feldmann, S. Göetzendoerfer, J. Meinhardt, G. Sextl, H. Kohlmann, S. Sedlmaier, W. Schnick and K. M. Buschbaum, *J. Am. Chem. Soc.*, 2013, **135**, 6896; (d) H. Qiao, Y. Jia, Y. Zheng, N. Guo, Q. Zhao, W. Lv and H. You, *CrystEngComm*., 2012, **14**, 5830; (e) W. F. Zhao, C. Zou, L. X. Shi, J. C. Yu, G. D. Qian and C. D. Wu, *Dalton Trans.*, 2012, **41**, 10091; (f) X. P. Zhang, D. G. Wang, Y. Su, H. R. Tian, J. J. Lin, Y. L. Feng and J. W. Cheng, *Dalton Trans.*, 2013, **42**, 10384; (g) S. R. Zhang, D. Y. Du, K. Tan, J. S. Qin, H. Q. Dong, S. L. Li, W. W. He, Y. Q. Lan, P. Shen and Z. M. Su, *Chem. – Eur. J.*, 2013, **19**, 11279; (h) C. Feng, J. W. Sun, P. F. Yan, Y. X. Li, T. Q. Liu, Q. Y. Sun and G. M. Li, *Dalton Trans*., 2015, **44**, 4640.

21 L. D. Carlos, R. A. S. Ferreira, V. Z. Bermudez and S. J. L. Ribeiro, *Adv. Mater.*, 2009, **21**, 509.

22 (a) L. D. Carlos, R. A. S. Ferreira, V. Z. Bermudez, B. Julián-López and P. Escribano, *Chem. Soc. Rev.*, 2011, **40**, 536; (b) Y. J. Cui, Y. F. Yue, G. D. Qian and B. L. Chen, *Chem. Rev.*, 2012, **112**, 1126; (c) S. Biju, Y. K. Eom, J. C. G. Buenzli and H. K. Kim, *J. Mater. Chem. C*, 2013, **1**, 3454.

23 S. Song, X. Li and Y.H. Zhang, *Dalton Trans.*, 2013, **42**, 10409.

24 M. L. Ma, C. Ji and S. Q. Zang, *Dalton Trans.*, 2013, **42**, 10579.

25 (a) M. L. P. Reddy and S. Sivakumar, *Dalton Trans.*, 2013, **42**, 2663; (b) N. M. Shavaleev, S. V. Eliseeva, R. Scopelliti and J. C. G. Bünzli, *Inorg. Chem.*, 2010, **49**, 3927.

26 A. J. Calahorro, A. S. Castillo, J. M. Seco, J. Zuñiga, E. Colacio and A. R. Diéguez, *CrystEngComm.*, 2013, **15**, 7636.

27 T. Smith and J. Guild, *Trans. Opt. Soc.*, London 1931, 33, 73.

28 G. M. Sheldrick, SHELXS-97: Programs for Crystal Structure Solution, University of Götingen: Götingen (Germany), 1997.

29 (a) H. Deng, Y. C. Qiu, Y. H. Li, Z. H. Liu, R. H. Zeng, M. Zeller and S. R. Batten, *Chem. Commun.*, 2008, 2239. (b) Y. C. Qiu, H. Deng, J. X. Mou, S. H. Yang, M. Zeller, S. R. Batten, H. H. Wu and J. Li, *Chem. Commun*., 2009, 5415. (c) G. Peng, Y. C. Qiu, Z. H. Liu, B. Liu and H. Deng, *Cryst. Growth Des.*, 2010, **10**, 114. (d) Y. C. Qiu, Y. H. Li, G. Peng, J. B. Cai, L. M. Jin, L. Ma, H. Deng, M. Zeller and S. R. Batten, *Cryst. Growth Des.,* 2010, **10**, 1332. (e) B. Liu, Y. C. Qiu, G. Peng and H. Deng, *CrystEngComm.*, 2010, **12**, 270. (f) Y. C. Qiu, Z. H. Liu, J. X. Mou, H. Deng and M. Zeller, *CrystEngComm*., 2010, **12**, 277.

(g) L. Ma, Y. C. Qiu, G. Peng, J. B. Cai, H. Deng and M. Zeller, *CrystEngComm*., 2011, **13**, 3852.
30 J. Q. Leng, H. F. Li, P. Chen, W. B. Sun, T. Gao and P. F. Yan, *Dalton Trans.*, 2014, **43**, 12228.
31 S. Raphael, M. L. P. Reddy, A. H. Cowley and M. Findlater, *Eur. J. Inorg. Chem*., 2008, **28**, 4387.
32 Q. Shi, R. Cao and M. C. Hong, *Trans. Met. Chem.*, 2001, **26**, 657.
33 K. Nakamoto, *Infrared and Raman Spectra of Inorganic and Coordination Compounds*, 3rd ed., Wiley, New York, 1978.
34 K. A. Cychosz and A. J. Matzger, *Langmuir*, 2010, **26**, 17198.
35 M. Kandiah, M. H. Nilsen, S. Usseglio, S. Jakobsen, U. Olsbye, M. Tilset, C. Larabi, E. A. Quadrelli, F. Bonino and K. P. Lillerud, *Chem. Mater.*, 2010, **22**, 6632.
36 S. J. Yang and C. R. Park, *Adv. Mater.*, 2012, **24**, 4010.
37 J. Duan, M. Higuchi, R. Krishna, T. Kiyonaga, Y. Tsutsumi, Y. Sato, Y. Kubota, M. Takata and S. Kitagawa, *Chem. Sci.*, 2014, **5**, 660.
38 J. Duan, M. Higuchi, S. Horike, M. L. Foo, K. P. Rao, Y. Inubushi, T. Fukushima and H. Kitagawa, *Adv. Funct. Mater.*, 2013, **23**, 3525.
39 I. Oueslati, R. A. Sá Ferreira, L. D. Carlos, C. Baleizão, M. N. Berberan-Santos, B. de Castro, J. Vicens and U. Pischel, *Inorg. Chem.*, 2006, **45**, 2652.
40 A. Y. Robin and K. M. Fromm, *Coord. Chem. Rev.*, 2006, **250**, 2127.
41 N. Sabbatini, M. Guardigli and J. M. Lehn, *Coord. Chem. Rev.*, 1993, **123**, 201.

Graphical Abstract

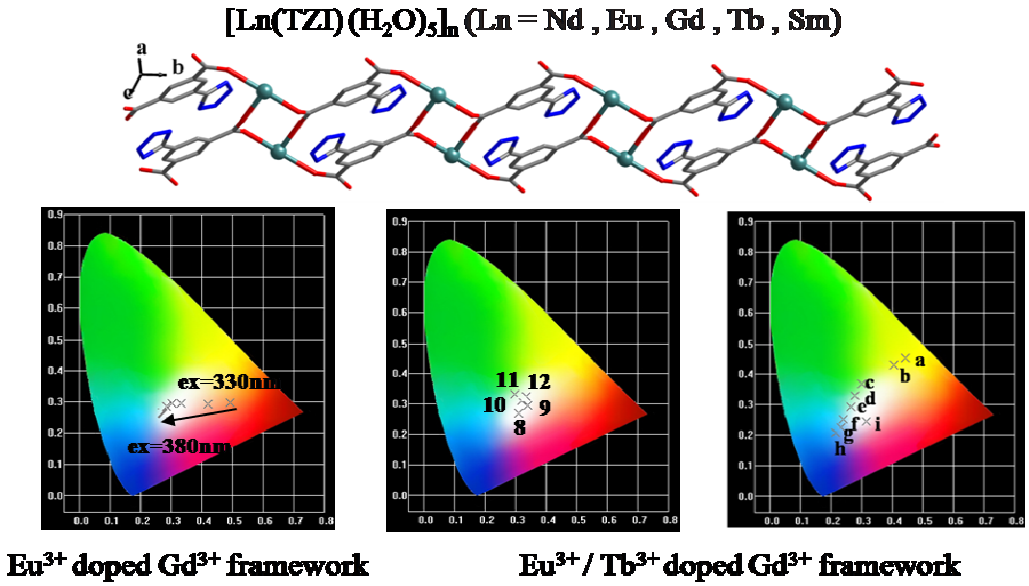

Eu^{3+} doped Gd^{3+} framework

Eu^{3+} / Tb^{3+} doped Gd^{3+} framework